Contrib Mineral Petrol (2016) 171:26
DOI 10.1007/s00410-016-1236-x

ORIGINAL PAPER

Preservation of primary mineral inclusions and secondary mineralization in igneous zircon: a case study in orthogneiss from the Blue Ridge, Virginia

Elizabeth A. Bell[1]

Received: 23 May 2015 / Accepted: 23 January 2016 / Published online: 27 February 2016
© Springer-Verlag Berlin Heidelberg 2016

Abstract A wide variety of minerals occur as inclusions in igneous zircon and can provide valuable evidence of source magma composition from originally magmatic zircons in metamorphic and clastic sedimentary rocks. However, it is not clear the extent to which zircons preserve the primary composition of their inclusions through a variety of geologic processes. This paper documents a case study of inclusion-rich, originally igneous zircon from an orthogneiss in the Blue Ridge of southwest Virginia. Zircon inclusions isolated from cracks contain 4 % clearly metamorphic phases (mainly in hosts with disturbed U–Pb systems) and otherwise retain distinct plagioclase chemistry, K-feldspar/plagioclase pairs, and biotite with much wider-ranging Mg/(Mg + Fe) than biotite in the rock matrix. A clearly secondary mineralization suite filling cracks in the zircons consists of quartz, biotite, albite, and epidote. Overall, these zircons preserve mineral inclusions distinct from their current host rock (except when exposed to external environments via cracks), demonstrating that non-metamict zircons may preserve their primary inclusion assemblages through later amphibolite to lower granulite facies metamorphism.

Communicated by Franck Poitrasson.

Electronic supplementary material The online version of this article (doi:10.1007/s00410-016-1236-x) contains supplementary material, which is available to authorized users.

✉ Elizabeth A. Bell
ebell21@ucla.edu

[1] Department of Earth, Planetary, and Space Sciences, University of California, Los Angeles, Los Angeles, CA, USA

Keywords Zircon · Mineral inclusion · Accessory minerals

Introduction

Zircon is a common accessory mineral in intermediate to felsic igneous rocks, and its physical and chemical hardiness mean that it also survives weathering and sedimentary transport in most cases (e.g., Fedo et al. 2003). The oldest dated terrestrial materials are detrital zircons from the Jack Hills, Western Australia, attesting both to the capacity of the mineral for preservation and to its importance in reconstructing crustal evolution over Earth history. As zircon crystallizes in a magma, it often traps exotic phases such as earlier-formed crystals and pockets of melt. Thus inclusions in detrital zircons are a valuable supplement to U–Pb dating in assessing their provenance. Inclusions in the Jack Hills zircons tend to be granitic in nature, including quartz, feldspar, and mica (Maas et al. 1992; Hopkins et al. 2010; Bell et al. 2011, 2015b). Although abundant carbonaceous phases were reported in Jack Hills zircons (Menneken et al. 2007; Nemchin et al. 2008), these were subsequently shown to be laboratory contamination (Dobrzhinetskaya et al. 2014). Subsequently, rare graphitic inclusions were documented in these zircons, but at a much lower incidence (<1 % of Hadean zircons; Bell et al. 2015a). Hopkins et al. (2008, 2010) applied thermobarometric methods to Hadean Jack Hills zircons containing muscovite or hornblende inclusions to infer their formation in a low heat flow environment, potentially suggestive of an underthrusting-type tectonic regime.

Although mineral inclusions in zircon potentially record diagnostic information about the magmatic environment in which the zircon formed, how accurately the mineralogy and chemistry of inclusions in detrital zircons can be used to

reconstruct zircon provenance is not entirely clear. Darling et al. (2009) determined that the mineral inclusions in zircons grown in intermediate to felsic melts within the Sudbury impact melt sheet consistently suggest a more felsic melt than the whole rock in terms of the modal proportions of quartz, alkali feldspar, and plagioclase. Jennings et al. (2011) also demonstrated that while the chemistry of igneous apatite and mafic phases is typically similar between crystals included in zircon and those in the whole rock, feldspar included in zircon is instead consistently higher in Or content and lower in An content than feldspar crystals in the whole rock. These results are consistent with the fact that zircon is often a late-crystallizing phase in high-temperature granitoids (Harrison et al. 2007), and thus more likely to capture other later-forming phases as inclusions.

Another major consideration is how well zircon can preserve the mineralogy and chemistry of its included phases. Although zircon is normally robust against chemical alteration, accumulated radiation damage can allow chemical alteration to the zircon crystal structure. Radiation-damaged regions typically develop microporosity and may swell, depending on the severity of the damage (e.g., Weber et al. 1993). Expansion of radiation-damaged regions in the crystal can result in cracking, providing a pathway for fluid ingress and alteration both along cracks and in radiation-damaged regions (e.g., Wayne and Sinha 1988). Cracks are recognized sites of chemical alteration and secondary mineralization within the Jack Hills zircons (Harrison and Schmitt 2007; Trail et al. 2007; Bell et al. 2015b). Rasmussen et al. (2011) investigated the inclusion record of the Jack Hills zircons and concluded based on comparison with the inclusion assemblages of various igneous zircon suites that the Jack Hills inclusions were largely secondary. However, Bell et al. (2015b) considered the Jack Hills inclusion suite with reference to likely alteration features and concluded that phases isolated from cracks in the host zircons were most likely primary, suggesting that fluid ingress into the zircon lattice away from cracks (e.g., into radiation-damaged regions) is minimal in the Jack Hills zircons.

Given the questions surrounding the robustness of zircon inclusion records, this paper presents a case study of inclusion-rich igneous zircons that have undergone later metamorphic events. The meta-igneous unit in question is a Grenville-aged biotite augen gneiss in the Blue Ridge of southwest Virginia which underwent several episodes of regional metamorphism during both the Grenville orogeny and various Paleozoic orogenies of the Appalachians, resulting in obvious chemical and textural alteration of the host rock. The modal mineralogy of the zircon inclusion suite was determined versus that of the rock matrix and the major element chemistry of silicate inclusions was measured for comparison to minerals in the rock matrix, in order to assess whether the inclusions have been isolated from the chemical changes occurring in the rock matrix or if they show similar modifications.

Samples and geological setting

Biotite augen gneiss samples (herein named "SVL") were collected from a railroad cut in Hardy, Virginia (N 37°13.517′, W 79°48.253′). The gneiss is mapped by Henika (2011) as a protomylonitic unit of the main gneissic lithofacies of the Horsepen Mountain Suite (Bartholomew 1981), consisting of granitoids intruded into Proterozoic gray gneisses of the Lovingston Massif during the Grenville orogeny ca. 1100–1000 Ma (Bartholomew 1981; Bartholomew and Lewis 1984). The Lovingston Massif was metamorphosed to amphibolite to lower granulite facies during the Grenville orogeny, with the timing of peak metamorphism in the area estimated as 1000–900 Ma (Bartholomew and Lewis 1984). Anorogenic granites intruded the Lovingston Massif during the late Proterozoic. The Stewartsville Pluton, ca. 1 km west of the sample site, is the closest example and has a zircon U–Pb age of 666 ± 10 Ma (Fokin 2003). Regional greenschist to amphibolite facies metamorphism occurred during Paleozoic orogenies (Bartholomew et al. 1981; Glover et al. 1982). Ages of regional metamorphism range from 480 to 340 Ma (Robinson 1976; Sinha 1976; Furcron 1969; Glover et al. 1982).

The SVL unit is a well-foliated biotite gneiss (Fig. 1) with cm-scale feldspar augen and larger, cm-scale leucosomes rich in K-feldspar, albite, and quartz. Examination in thick section reveals inter-grown biotite and quartz interspersed with cm-scale albite in the melanocratic matrix (Fig. 2a). Albite in the melanocratic matrix typically contains small crystals of epidote (and more rarely muscovite) on the 10 s of μm scale and is often surrounded by fine-grained muscovite (Fig. 2b), all features suggesting feldspar alteration. Apatite, ilmenite, and titanite are also abundant. Leucosomes contain elongated, rounded grains of feldspar and quartz (Fig. 2e, f). K-feldspar in leucosomes displays perthitic association with albite (Fig. 2c) and also appears to be replaced by albite in the outer regions of many crystals (Fig. 2e, f). Quartz, apatite, less abundant biotite, ilmenite, titanite, and (apparently secondary) muscovite surrounding the feldspars are also present in leucosomes. Zircon is found in accessory amounts in both leucosomes and the dominant melanocratic matrix. Titanite characteristically mantles ilmenite in both leucosome and melanocratic matrix (Fig. 2b, d).

Materials and methods

Samples were processed by crushing and sieving to <425 μm followed by elution in water and heavy liquid

Fig. 1 Several views of the SVL gneiss in outcrop

separation. For SVL gneiss, the melanocratic main portion (SVL1a/SVL1D) and leucosomes (SVL1c/SVL1L) were processed separately. Separated zircons were mounted in epoxy and polished with silicon carbide grit to expose their interiors. Thick sections of each sample were also prepared, mounted in epoxy, and polished with silicon carbide grit. Separately, powders of the melanocratic matrix and leucosomes were analyzed by X-ray Fluorescence at the Pomona College XRF Laboratory.

Zircon mounts were imaged by cathodoluminescence (CL) to reveal internal textures and classified as Magmatic, Altered, "Altered Magmatic," and Ambiguous. For the purposes of this study, magmatic zoning is defined by the presence of fine oscillatory zoning (e.g., Corfu et al. 2003). Because not all magmatic zircons will display primary oscillatory zoning, this approach may miss some magmatic zircons with unaltered zoning. Altered zircons show zoning which is not oscillatory in nature and may be patchy (e.g., Corfu et al. 2003) or cloudy and diffuse. The Altered Magmatic category includes grains with remnant oscillatory zoning which has been overprinted or blurred in places. Ambiguous grains are mostly dark and homogeneous. Examples of magmatic and variably altered CL zoning patterns are shown in Fig. 3. Backscattered electron (BSE) imaging and semiquantitative energy-dispersive X-ray spectroscopy (EDS) analyses were used to find and tentatively identify inclusions in zircon. These inclusions were then targeted for quantitative compositional analysis by electron probe microanalysis (EPMA). All identified inclusions are listed in Table S1 of the online supplement.

Ti–U–Th–Pb analysis

Zircons were analyzed for U–Pb age and the contents of several trace elements on a CAMECA *ims*1270 ion microprobe using the Ti–U–Th–Pb protocol of Abbott et al. (2012) adapted for spot mode. This analytical protocol combines U–Th–Pb isotopic analysis (e.g., Mojzsis et al. 2003) with abundance measurements of the trace elements Ti, Y, U, and Th and the minor element Hf. A primary O^- beam with current ca. 10–15 nA was focused to a ca. 30 μm diameter spot. U–Th–Pb calibration utilized the AS3 zircon standard (Paces and Miller 1993), and trace element calibration utilized the 91500 zircon standard abundances of Wiedenbeck et al. (2004) for Y, Hf, Th, and U, along with the Ti abundance reported by Fu et al. (2008). After ion probe analysis, samples were re-imaged by secondary electron (SE) and BSE imaging to check for cracks or inclusions overlapping the ion probe pits. Only concentration results from spots not overlapping cracks or inclusions were included in the discussion or figures, given the danger of contamination by phases filling cracks (e.g., Harrison and Schmitt 2007). U–Th–Pb isotopic analyses from these spots are still considered. The analyses were completed in two sessions. All ion microprobe data are tabulated in Table S1 of the supplemental materials.

EPMA analysis

Non-quartz silicate inclusions identified by EDS were analyzed for quantitative stoichiometry on a JEOL-8600 electron microprobe, using a ~1-μm spot (in order to analyze small inclusion phases) at 20-kV accelerating voltage. Most inclusions were imaged by beam mapping prior to quantitative analysis in order to further identify separate minerals in multiphase inclusions. Mica, feldspar, and other phases from both the melanocratic matrix and the leucosomes were also analyzed in thick section under the same conditions. Only analyses with oxide totals >90 % were considered, and effects of secondary fluorescence in the zircon host were accounted for by subtraction of Zr from the

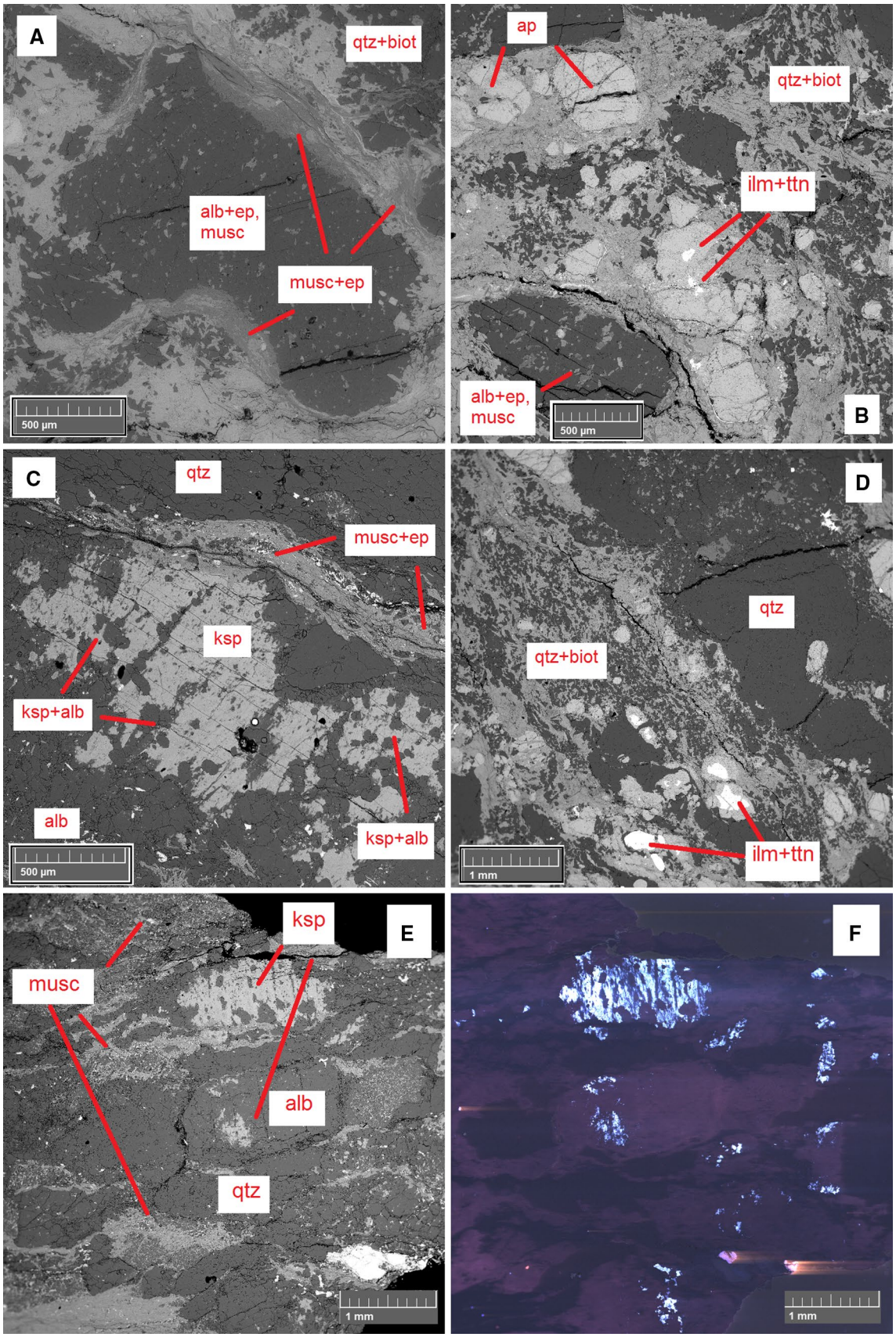
A
qtz+biot
alb+ep,
musc
musc+ep
500 µm
ap
qtz+biot
ilm+ttn
alb+ep,
musc
500 µm
B
C
qtz
musc+ep
ksp
ksp+alb
alb
500 µm
ksp+alb
D
qtz
qtz+biot
1 mm
ilm+ttn
ksp
E
musc
alb
qtz
1 mm
F
1 mm

◀**Fig. 2** Backscattered electron (BSE) and color cathodoluminescence (CCL) images of thick sections from the melanocratic matrix and leucosomes. **a**, **b**, **d** Melanocratic matrix showing quartz + biotite association and albites with associated epidote and muscovite. **c** K-feldspar and albite in perthitic association in a leucosome. **e**, **f** Wider view of a leucosome showing rounded grains of feldspar and quartz. **e** BSE, **f** CCL. K-feldspar exists in small perthitic patches within larger grains of albite. *Qtz* quartz, *ksp* K-feldspar, *alb* albite, *ilm* ilmenite, *ttn* titanite, *ap* apatite, *musc* muscovite, *ep* epidote

results along with the appropriate corresponding Si signal for zircon. Phyllosilicates were renormalized to 95 total wt% and other phases to 100 wt%. Cation counts were calculated assuming 22 oxygens for micas and 8 oxygens for feldspars. All stoichiometric data and calculations are collected in Table S2 of the online supplement. Representative X-ray maps of small multiphase feldspar inclusions are shown in Fig. S3 of the online supplement.

Results

Whole-rock chemistry for SVL1D and SVL1L is shown in Table 1. Zircons from both are indistinguishable in U–Pb systematics and trace chemistry and generally record Grenville U–Pb ages, a range in trace element contents, and a granitic inclusion suite. Most zircons display magmatic oscillatory zonation or variably altered and overprinted magmatic zonation under CL imaging (Fig. 3). Most inclusions are isolated from cracks in the zircon surface and occur in both magmatically zoned and altered regions.

SIMS Ti–U–Th–Pb results

Zircons that are concordant within 2σ age error (calculated using the $^{207}Pb/^{206}Pb$ vs. $^{206}Pb/^{238}U$ ages) have $^{206}Pb/^{238}U$ ages ranging from 1216 to 807 Ma with a weighted mean

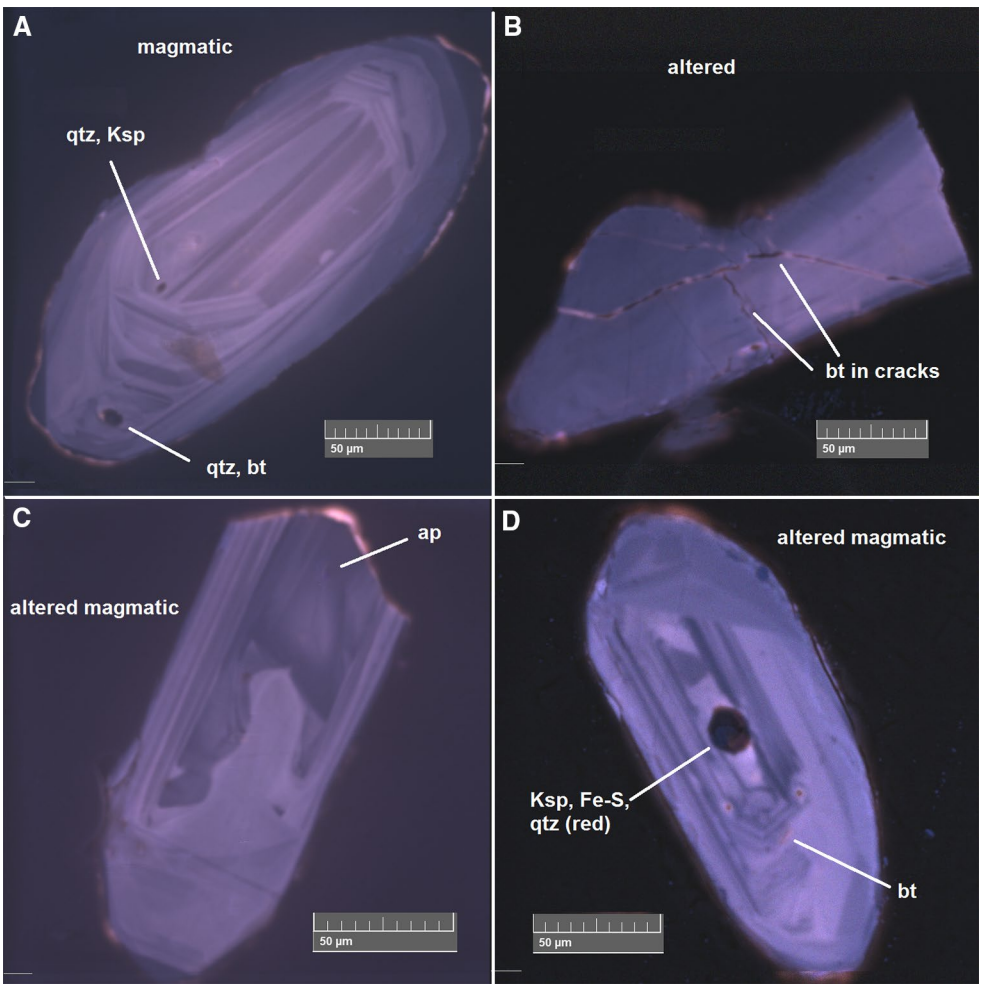

Fig. 3 Examples of zircon CL zoning patterns. **a** Unaltered magmatic zoning in sample SVL1c-3.10, **b** altered pattern with no magmatic zoning still visible in SVL1a-7.3, **c**, **d** magmatically zoned zircons (SVL1c-7.1 and SVL1a-1.6, respectively) with some alteration, called "altered magmatic" in Table S1. Inclusions in altered regions are so marked in Tables S1–S2

Table 1 XRF data for the main, melanocratic matrix of the SVL gneiss (SVL-1D; yielding SVL-1a zircons) and for leucosome material (SVL-1L; yielding SVL-1c zircons). Total Fe is reported as Fe_2O_3

	Melanocratic	Leucosome
Oxide wt%		
SiO_2	62.70	74.59
TiO_2	1.85	0.41
Al_2O_3	14.43	13.76
Fe_2O_3 (tot)	7.52	1.97
MnO	0.12	0.02
MgO	1.61	0.29
CaO	4.25	2.33
Na_2O	3.64	4.47
K_2O	2.59	1.71
P_2O_5	0.96	0.21
Total	99.67	99.75
ppm		
Rb	73	24
Sr	383	379
Ba	910	1333
Zr	616	191
Y	65	18
Nb	32	0
Cs	0	0
Sc	16	5
V	86	26
Cr	12	13
Ni	0	0
Cu	2	0
Zn	176	28
Ga	20	20
La	49	25
Ce	141	40
Pr	21	5
Nd	89	23
Hf	15	5
Pb	24	10
Th	0	0
U	0	4

of 1020 ± 13 Ma (2σ; MSWD = 0.79). Twelve out of the 98 U–Pb analyses yield discordant ages (age disagreement larger than age error) ranging from +18 to −48 % discordance. The cause of reverse discordance is not immediately clear given the relatively low U contents. Given the range in concordant ages, some zircons may have experienced significant Pb loss during Grenville orogenesis or were inherited, but no clear upper and lower intercepts could be distinguished. Figure 4 shows a Concordia diagram for zircons separated from the melanocratic matrix and leucosomes. The two populations do not differ significantly

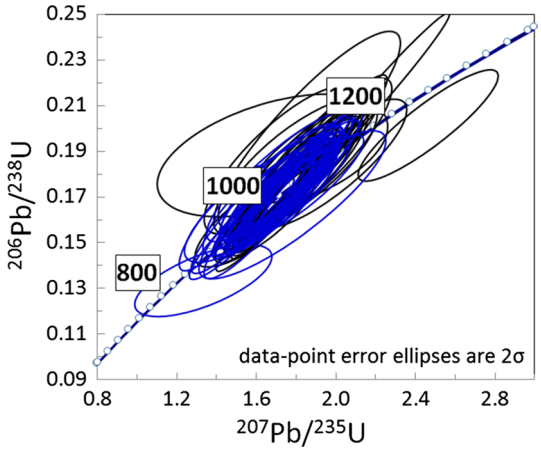

Fig. 4 Concordia plot for zircons from melanocratic matrix (*black*) and leucosomes (*blue*). There is no systematic difference between the two groups. Twenty-two data points with >20 % error on U–Pb ages are omitted from this graph but included in Table S1 of the online supplement

in age or discordance, despite the melanocratic matrix containing a higher proportion of zircons with CL zonation altered beyond the point of recognizing originally magmatic features. Unsurprisingly, 10 out of 12 discordant grains fall into the "altered" or "altered magmatic" categories. Age and trace element data are provided in Table S1.

Trace element data are shown in Fig. 5. Given knowledge of rutile activity (uncertain in the magma), the Ti concentration in zircon can be used as a crystallization thermometer (Watson and Harrison 2005). Average Ti contents in the zircons are 25 ± 32 ppm (1 SD). Assuming $\alpha_{TiO_2} = 1$, the zircons' average crystallization temperature is 803 ± 66 °C (1 SD). If a lower α_{TiO_2} of ~0.7 would be more appropriate, then this would underestimate the true crystallization temperatures by ~50 °C (Watson and Harrison 2005). Given the uncertainty in the original magma α_{TiO_2}, Ti contents rather than calculated temperatures are reported in figures. (Th/U) ratios of 0.54 ± 0.15 (1 SD) resemble common magmatic values. Concentrations of Hf and Ti and the ratio Th/U typically show trends within magmatic zircon populations reflecting melt compositional evolution: Hf increases while Th/U and Ti decrease (Claiborne et al. 2010). SVL zircons display the expected inverse Th/U versus Hf trend (Fig. 5d), but Ti displays no apparent trends with other trace element quantities (e.g., Fig. 5c). U contents are moderate, averaging 175 ± 122 ppm (1 SD) (Fig. 5b). There are few differences in trace element contents and ratios among CL zonation categories in this population or between matrix and leucosome zircons. Although trace elements show no clear trends with % discordance or age (Fig. 5a, b), several zircons with high common Pb (defined as <98 % radiogenic ^{206}Pb)—a potential outcome of fluid-involved alteration (e.g., Hoskin and Schaltegger

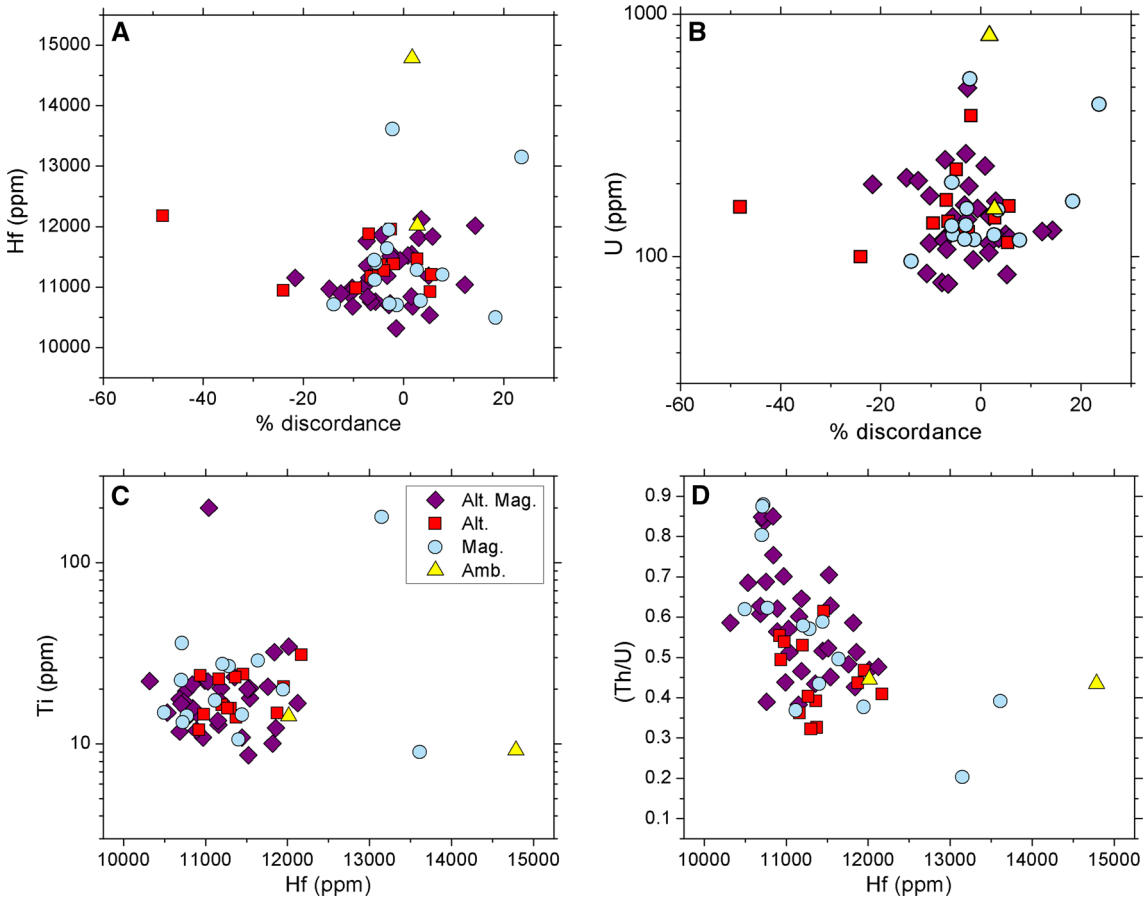

Fig. 5 Trace element contents in the host zircons, categorized by CL zoning style. **a** Hf versus % discordance, **b** U versus % discordance, **c** Ti versus Hf, **d** Th/U versus Hf. Th/U and Hf display the negative correlation often resulting from magmatic compositional evolution (e.g., Claiborne et al. 2010), while Ti does not show clear correlations with other trace elements. The studied trace elements do not show systematic variations with age. *Alt.*: altered; *Alt. Mag.*: altered magmatic; *Mag.*: magmatic; *Amb.*: ambiguous. Average 1σ *error bars* Th/U, 0.1; Ti, 2 ppm; Hf: 610 ppm

2003)—do have unreasonably high Ti contents (corresponding to >1075 °C) for zircons in granitoids with SVL's Zr contents (see, e.g., Boehnke et al. 2013). This is much higher than the rest of the population and likely an alteration effect.

Inclusion occurrence and chemistry

SVL zircons contain both single- and poly-phase inclusions, dominated by quartz, feldspar, and biotite. The majority are not obviously associated with cracks ("isolated"), while others are found intersecting or filling cracks. Examples of these textures are shown in Fig. 6. Isolated inclusions occur within regions of altered as well as unaltered magmatic zoning. Modal mineralogy of the inclusions varies with relationship to cracks (Fig. 7a), but not with either relationship to zoning style (Fig. 7b) or melanocratic versus leucosome origin (Fig. 8). Isolated inclusions display little relationship to host zircon age or U–Pb disturbance except for the presence of chlorite, muscovite, and epidote mostly in grains with high common Pb (Fig. 9). Biotite varies widely in Mg/(Mg + Fe) (Mg#) and Ti_{apfu} (Fig. 10). K-feldspar, albite, and plagioclase are present (Fig. 11). K-feldspar and plagioclase are often found in the same polyphase inclusion (perthitic association or "Psp" in figures) among the isolated suite but not among the on-crack or crack-filling suites. Beam mapping often revealed that small isolated feldspar inclusions contain both K-feldspar and plagioclase too small to definitively resolve by EPMA, and these analyses are shown in Fig. 11 but not included in discussions of plagioclase chemistry. Although their ranges overlap, isolated plagioclase ranges more calcic than plagioclase in the crack-filling or—intersecting suites or in the rock matrix. Other phases not included on Figs. 7 and 8 are listed in Table S1 and include rare Fe sulfide and several instances of Fe–Al-rich phases not amenable to EPMA (potentially small biotite or chlorite inclusions).

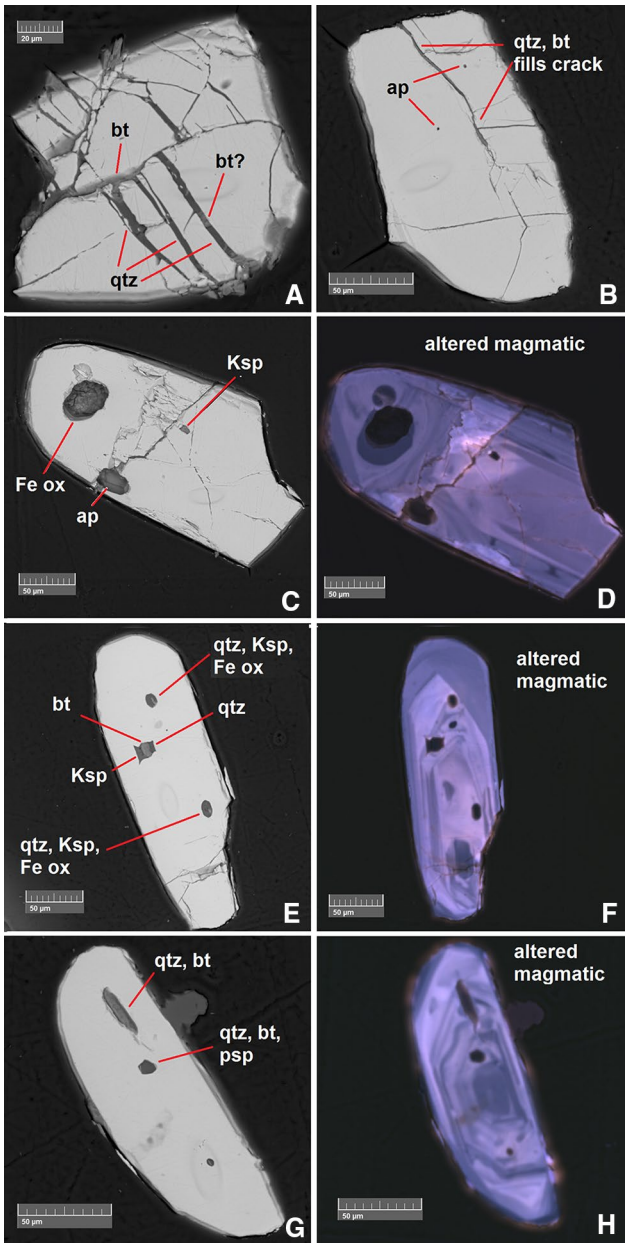

Fig. 6 Examples of inclusions with various relationships to cracks. **a**, **b** BSE images of phases filling cracks in samples SVL1a-3.1b and SVL1c-8.4, respectively, **c**, **d** BSE and CL images, respectively, of isolated and crack-intersecting inclusions in SVL1a-4.8, **e**, **f** BSE and CL images, respectively, of isolated inclusions in SVL1c-7.5, **g**, **h** BSE and CL images, respectively, of isolated and crack-intersecting inclusions in SVL1c-4.5. *Qtz* quartz, *Ksp* K-feldspar, *Psp* perthitic-textured feldspar, *Ap* apatite, *Fe ox* Fe oxide, *Bt* biotite

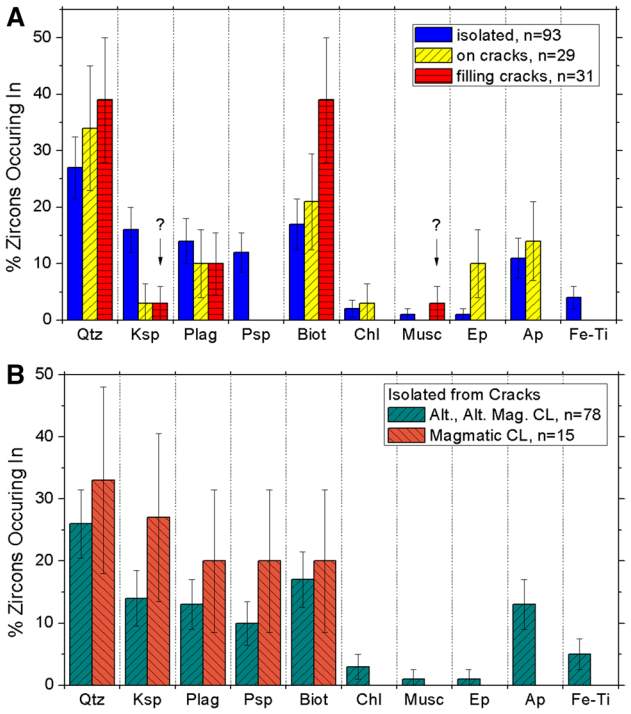

Fig. 7 Modal mineralogy of inclusions in the zircons. **a** Categorized by relationship to cracks, **b** inclusions isolated from cracks categorized by the CL zoning in the region in which they reside. *Qtz* quartz, *Ksp* K-feldspar, *Plag* plagioclase, *Psp* perthitic-textured feldspar (not considered in total), *Musc* muscovite, *Biot* biotite, *Chl* chlorite, *Ep* epidote, *Ap* apatite, *Fe–Ti* Fe–Ti oxide, undifferentiated. *Error bars* are 1σ based on counting statistics

Discussion

Zircons in the SVL orthogneiss have ages reflecting Grenville crystallization, are largely concordant, and appear to have magmatic Ti contents, Th/U, and originally magmatic (although mostly later altered) CL zoning. The zircons are rich in mineral inclusions, and the inclusions have a variety of associations with textural features such as cracks and style of CL zoning. Since cracks are a likely pathway for fluid ingress into zircons, they are likely sites of alteration or chemical exchange with the outside environment, and cracks often form in zircon during deformation. The age and moderate U contents of the zircons mean that most are unlikely to have been amorphized by radiation damage even absent any thermal annealing since their formation (see e.g., Garver and Kamp 2002), limiting the opportunities for fluid ingress into uncracked regions of most zircons. However, blurred and faded or otherwise altered CL zoning in some regions attests to some processes altering the zircons, despite the lack of clear differences in trace element contents, and high common Pb may also suggest alteration in a few grains.

The zircons thus present a useful case study for the behavior of igneous zircon mineral inclusions during metamorphism and in zircons that have apparently undergone various degrees of alteration by multiple mechanisms. The role of textural features such as cracks in facilitating

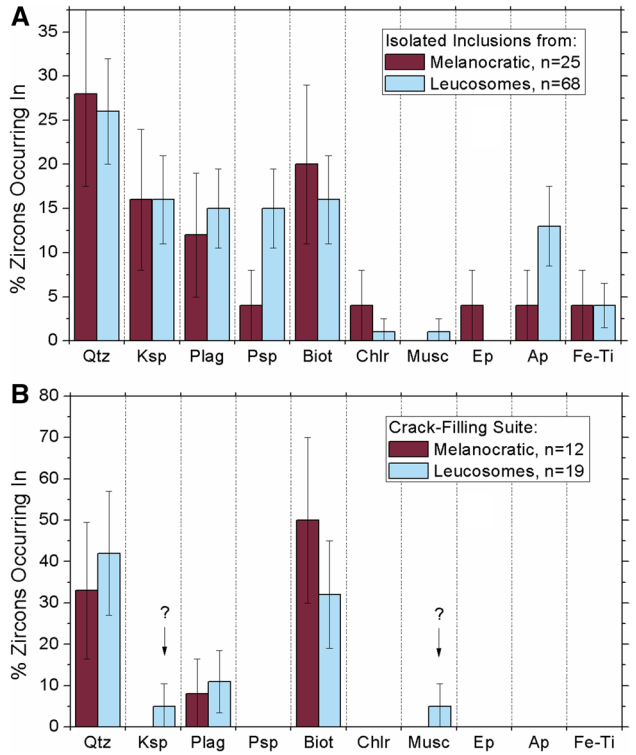

Fig. 8 Modal mineralogy of inclusion suites by region of the rock their host zircons resided in. **a** Isolated inclusions, **b** crack-filling inclusions. Major differences are not apparent between melanosome and leucosome zircons. Abbreviations as for Fig. 7 caption. *Error bars* are 1σ based on counting statistics

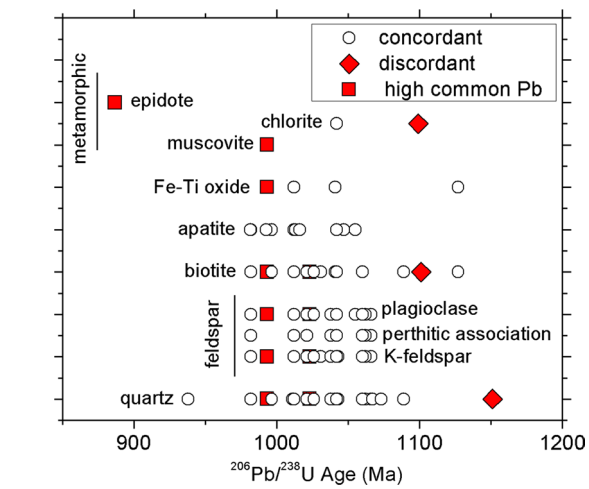

Fig. 9 Occurrence of isolated inclusions by host zircon age, categorized by U–Pb systematics. "Concordant": concordant within age error; "Discordant": discordant within age error; "High common Pb": <98 % radiogenic ^{206}Pb regardless of concordancy (another potential sign of alteration)

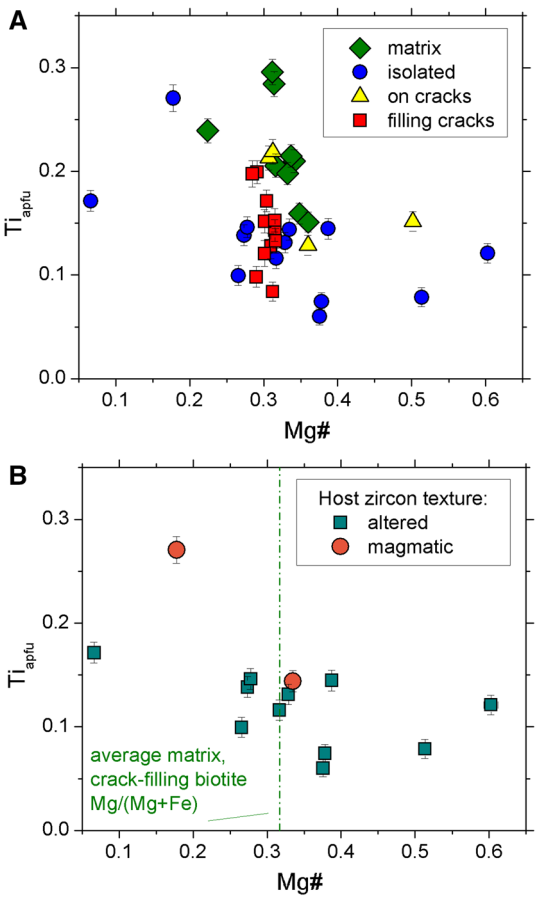

Fig. 10 Biotite chemistry variations, categorized by relationship to potential alteration features in the host zircon. **a** Matrix biotite and biotite inclusions categorized by relationship to cracks, **b** isolated biotite inclusions categorized by CL zoning of their host zircon (*altered* category includes both altered and altered magmatic). Mg# = Mg/(Mg + Fe) based on cation ratio; Ti_{apfu} normalized to 22 oxygens. *Error bars* are 1σ

inclusion alteration was examined, along with the potential for preservation of primary inclusions in both disturbed and undisturbed regions of the zircon crystal.

Do inclusions reflect the present whole rock?

Following high-temperature Grenville metamorphism (Bartholomew and Lewis 1984), rocks of the Blue Ridge were metamorphosed to greenschist or amphibolite facies during several Paleozoic orogenies (Bartholomew et al. 1981; Glover et al. 1982). Plagioclase grains in the melanocratic matrix contain small regions of epidote and muscovite. Albite and K-feldspar in both the leucosomes and matrix are often surrounded by a layer of muscovite ± epidote. Both features are likely a product of metamorphism or

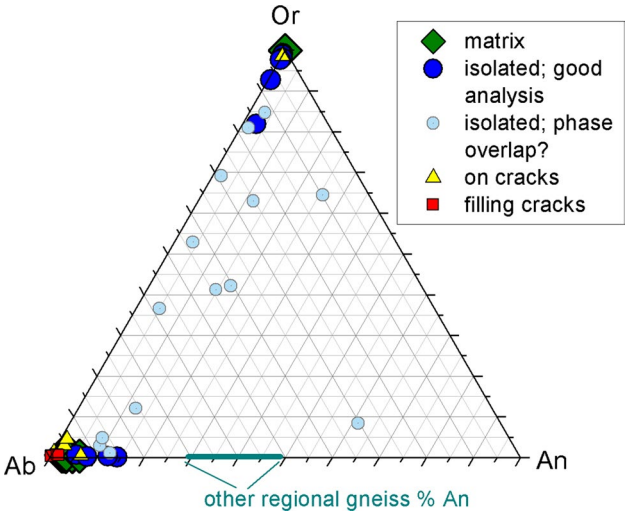

Fig. 11 Chemistry of matrix and inclusion feldspar, with inclusion feldspars categorized by their relationship to cracks in the host zircons. Isolated feldspars with small phases potentially overlapped by the electron microprobe beam (as determined by beam mapping) are shown if their K + Na + Ca cation total is >0.5 (ideal for normalization to 8 oxygens is 1.0). Other regional gneiss plagioclase % An from Bartholomew (1981)

other aqueous alteration. K-feldspar is present and is nearly pure orthoclase, with perthitic intergrowths of albite (see Fig. 2). The major constituents biotite and albite have a small compositional range in the whole rock, likely reflecting growth or equilibration during later alteration. Biotite and feldspar chemistry differ between the inclusions and the whole rock (Figs. 10, 11), while modal proportions of various mineral inclusions display a strong relationship with cracks in the host zircon (Fig. 7). The mineralogy of the isolated inclusion suite does not differ substantially with the position of the zircon in the present rock—those separated from leucosomes and from the melanocratic portion of the rock are highly similar (Fig. 8a). The crack-filling assemblage likewise shows little difference with location in the present whole rock (Fig. 8b).

Likely alteration phases and relationship to textural features

Some phases are clearly secondary, filling void space along cracks. This secondary suite, like the whole rock, is dominated by quartz and biotite. Nearly pure albite is a minor component, and a single K–Al–Si-bearing inclusion is also seen (although not measured by EPMA and thus indistinguishable between K-feldspar and muscovite). Albite in the crack-filling assemblage is similar in chemistry, although slightly less calcic than that in the rock matrix, averaging 0.8 ± 0.8 % An (1 SD), while the matrix plagioclase averages 3.5 ± 1.2 % (1 SD) An. Crack-filling biotite compares well to matrix biotite in Mg#: Both show a limited range compared to other biotite inclusions (Fig. 10). Crack-filling biotite has similar but slightly lower Ti contents than biotite in the whole rock. Three out of five measured crack-intersecting biotite inclusions fall within this range of matrix and secondary biotite compositions. Biotite isolated from cracks, even that in regions with disturbed CL zoning, varies widely in both quantities, although their average Mg# of 0.33 ± 0.14 (1 SD) is similar to that of the matrix and secondary phases (0.31 ± 0.03, 1 SD). In certain rocks, the Ti content of biotite can be used as a geothermometer (Henry and Guidotti 2002). In the strict sense, application of the thermometer requires a metapelite containing graphite, an aluminous phase, and either rutile or ilmenite (Henry et al. 2005); of these phases, only ilmenite is present in the SVL orthogneiss. The Ti contents of matrix biotites would suggest an average Ti-in-biotite temperature ~570 °C. However, the lack of an aluminous phase in the rock renders this likely an overestimate of temperature. In the absence of information about the granitoid protolith's accessory mineralogy, the significance of the similar Ti contents among isolated biotite inclusions in zircon is unclear, as this is relatively low for magmatic biotite.

Epidote and muscovite, secondary phases seen in the rock matrix, are not observed filling cracks. However, three epidote inclusions and one chlorite inclusion occur intersecting cracks (~10 % of crack-intersecting phases), while one muscovite, one epidote, and two chlorite inclusions occur among the isolated assemblage (~4 % of isolated phases), all in regions of altered CL zoning and all but one in zircons with relatively high common Pb (indicating potential disturbance to the U–Pb system). Nearly pure albite may exist only or mostly as a secondary phase in the zircons, given its rarity in the isolated suite compared to more calcic plagioclase compositions and its presence along and filling cracks (Fig. 11). Many phases found in the secondary suite (quartz, biotite) and other alteration-related species are much less common among the isolated assemblage, such that overall mineralogical evidence for inclusion replacement or alteration correlates well with the presence of cracks but not with other indicators of zircon alteration such as altered CL zoning.

Isolated inclusions

The isolated inclusion suite contains four instances of clearly secondary, metamorphic minerals (mostly in U–Pb-disturbed regions), but also preserves feldspar and biotite chemistries that differ from their counterparts in the rock matrix (Figs. 10, 11). Isolated biotite inclusions range more widely in Mg# and have slightly lower Ti_{apfu} than matrix biotite, although their ranges overlap substantially. Isolated

plagioclase (9.9 ± 4.1 % An, 1 SD) is more calcic than matrix plagioclase (3.5 ± 1.2, 1 SD), although some overlaps do occur between the two suites.

Most isolated feldspars occur in multiphase inclusions containing both K-feldspar and plagioclase. Beam mapping of small (<5 μm) feldspar inclusions on the electron microprobe was used to distinguish inclusions with small-scale separations (likely, exsolution) of K-feldspar and plagioclase, many with separate phases too small to be analyzed individually by EPMA. Inclusions with paired plagioclase and K-feldspar are shown in Figs. 7, 8 and 9 as perthitic feldspar ("Psp") and the phases counted separately as plagioclase and K-feldspar. As expected, their compositions are mostly consistent with varying mixtures between K-feldspar and relatively sodic plagioclase (with two more Ca-rich exceptions). Given the generally high estimated Ti temperatures for this zircon suite, it is likely that these inclusions were initially captured as single homogeneous phases which subsequently exsolved. Perthitic and single-phase feldspar inclusions occur in both magmatic and disturbed CL zoning within their host zircons, showing no clear correlation between zircon disturbance and feldspar exsolution history.

Greenschist facies overprinting in the matrix and zircons

Likely altered or secondary inclusion phases correlate well with presence along cracks. Among the isolated assemblage, they are usually found in U–Pb-disturbed regions. Overall, the isolated assemblage contains 4 % clearly metamorphic as well as potentially magmatic phases in the isolated suite in regions with disturbed CL zoning. This suggests that fluid ingress and consequent reactions along cracks were the primary mode of inclusion alteration, with regions of zircon away from cracks for the most part unaffected. This conclusion is supported by the maintenance of magmatic trace element contents in those unaltered regions and their relatively low U contents (i.e., leading to only minor radiation damage). Metasomatism of granitic rocks can lead to a variety of mineralogic changes, including quartz dissolution and albitization of feldspars (e.g., Cathelineau 1986; Plumper and Putnis 2009; Engvik et al. 2008). The secondary mineralizing assemblage seen among the zircons (mainly quartz, biotite, albite) also constitutes the major phases in the present rock matrix with its greenschist facies overprint.

The greater abundance of albite both intersecting and filling cracks suggests that most feldspar in contact with fluids along the cracks has been albitized in situ, consistent with the generally albitic compositions of plagioclase formed at greenschist facies (e.g., Spear 1995). The higher proportion of epidote among crack-intersecting than crack-isolated phases also suggests its formation by alteration of the previous inclusion phase (probably plagioclase). The proportions of quartz, biotite, and apatite do not differ appreciably between the crack-isolated and crack-intersecting assemblages, suggesting no preferential destruction of these phases along cracks. These phases are common in the current host rock and likely to have been present in the protolith (based on its being a continental granitoid), so it is not surprising that they would have remained stable during alteration. The persistence of larger K-feldspar suggests that albitization was incomplete, while smaller K-feldspar inclusions in zircon were mostly altered.

Neither the zircons' isolated nor secondary inclusion assemblages differ with origin in the melanocratic versus the leucosome portions, and the secondary suite is similar to major phases (quartz, biotite, albite) present in all parts of the rock, suggesting a similar mineralization history. Albitization of many on-crack feldspar inclusions and precipitation of albite, quartz, and biotite along cracks in the zircons probably occurred during greenschist facies overprinting of the SVL gneiss.

Preservation of primary inclusions

Following the formation of the SVL gneiss protolith, the Lovingston Massif underwent amphibolite to lower granulite facies metamorphism during the Grenville orogeny (Bartholomew and Lewis 1984). The large spread in U–Pb ages and presence of discordant zircons may suggest Pb loss in some of the zircons during this event. Overprinting at greenschist to amphibolite facies during late Precambrian to Paleozoic orogenies (Glover et al. 1982) is reflected in the mineral assemblage and highly sodic nature of the plagioclase both in the present rock matrix and along cracks in the zircons. Several instances of the metamorphic minerals chlorite, epidote, and muscovite among the isolated assemblage suggest that at least some metamorphic overprinting is reflected in this suite. However, the contrasting compositions between feldspar in this secondary suite and the isolated assemblage suggests that the isolated feldspar inclusions were not overprinted by the greenschist facies metamorphism. The biotite's wider range in Mg# suggests a similar independence from the greenschist facies overprint (although low Ti contents similar to that in the present matrix complicate the picture). However, it is necessary to consider whether these feldspar compositions and the biotite Mg# reflect original magmatic compositions or overprinting during granulite grade metamorphism.

Feldspars

The distinct compositions and textures of isolated feldspar inclusions are not in equilibrium with feldspars in the current whole rock. Secondary feldspar filling cracks in the

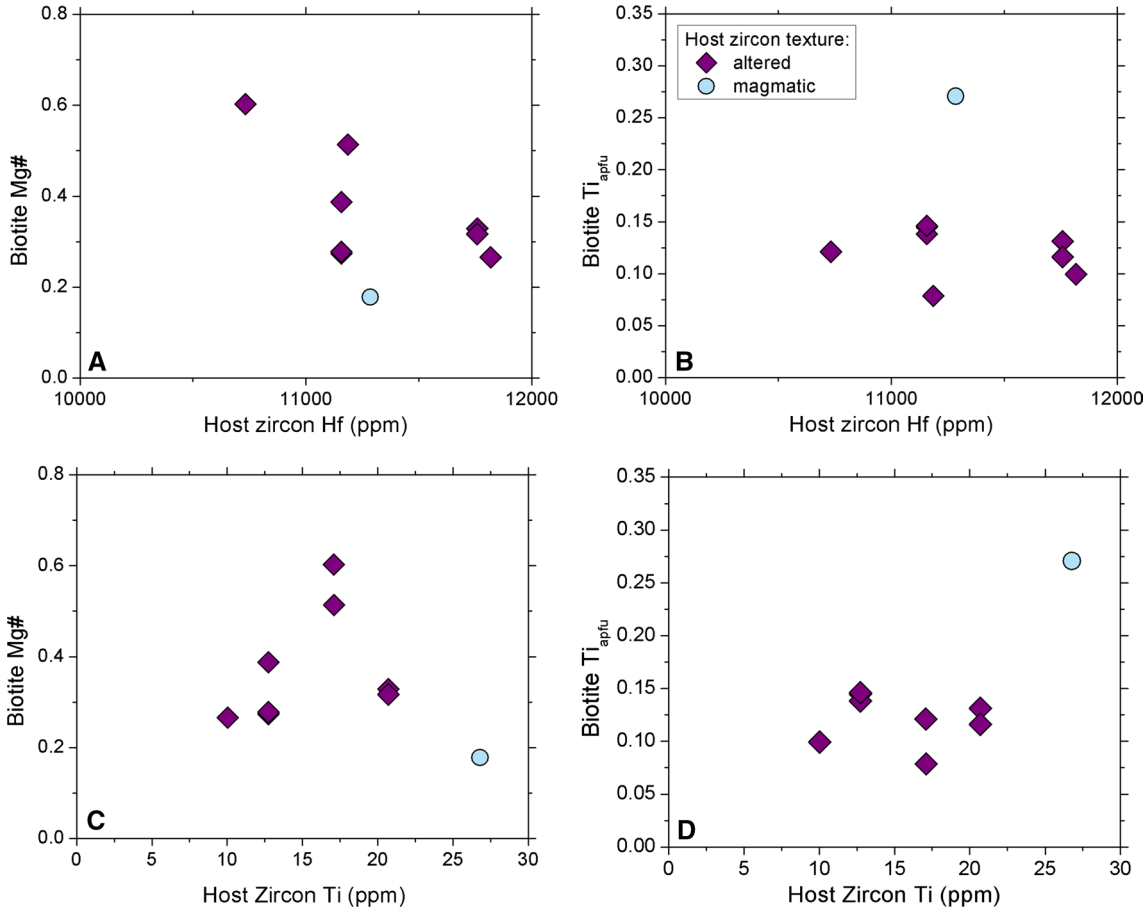

Fig. 12 Chemistry of isolated biotite inclusions versus host zircon chemistry. **a** Biotite Mg# versus host zircon Hf, **b** biotite Ti_{apfu} versus host zircon Hf, **c** biotite Mg# versus host zircon Ti, **d** biotite Ti_{apfu} versus host zircon Ti. Although Mg# shows a trend with Hf potentially indicative of evolving melt chemistry, other such chemical measures show no characteristic trends. *Altered* category: both altered and altered magmatic

zircons, the likely albitized feldspar inclusions that intersect cracks, and plagioclase in the whole rock are highly sodic and consistent with the greenschist facies overprint. Since there is no sample of the unmetamorphosed protolith for comparison, it cannot be definitively established that no change has affected the isolated feldspars' bulk compositions. However, plagioclase in the isolated assemblage resembles neither the greenschist overprint nor plagioclase in the higher-grade Blue Ridge units which the SVL gneiss likely resembled before its overprinting. Granulite gneisses in the Lovingston and Pedlar massifs alike contain far more calcic plagioclase (Bartholomew 1981 reports An_{32} to An_{50}), consistent with the higher-grade metamorphism (e.g., Spear 1995) and offset from the more sodic compositions of the isolated inclusions (An_5 to An_{14}) as well as the on-crack, crack-filling, and matrix albites (An_0 to An_6).

Any equilibration with the environment outside the zircons must have occurred well before the establishment of the present feldspar composition in the rock and is unlikely to have occurred during the high-temperature Grenville metamorphism given the more sodic plagioclase compositions. In addition, there are no significant differences in the distribution of isolated K-feldspar, plagioclase, or perthitic K-feldspar/plagioclase pairs between regions of zircon with magmatic CL zoning versus altered CL zoning. It is therefore most likely that isolated feldspar inclusions retain their primary magmatic bulk compositions.

Biotite compositions

The widely varying compositions among isolated biotite inclusions are not all in equilibrium with biotite in the present whole rock (Fig. 10). Crack-filling biotite, however, is similar to the average composition of the whole rock in both Mg# and Ti_{apfu} (Fig. 10). Isolated inclusions in both magmatically zoned and CL-altered regions of zircon display Mg# far more variable than the secondary and matrix biotite, although similar in average values (Fig. 10). It is

therefore unlikely that the isolated biotite Mg# represents the greenschist facies overprinting of the SVL gneiss, but the effects of high-temperature metamorphism require evaluation. Because primary biotite inclusions in zircon tend to be similar to host granitoid biotites in composition (Jennings et al. 2011), the wide range of compositions shown by the isolated biotite inclusions is difficult to interpret in terms of protolith biotite chemistry. However, since biotite Mg# decreases with increasing host zircon Hf in these zircons (Fig. 12), and since zircon Hf content increases characteristically with magma cooling and compositional evolution (Claiborne et al. 2010), this could be interpreted as the capture of biotite with progressively changing Mg# with magma compositional evolution. However, this interpretation is complicated by the lack of a clear trend in Mg# with host zircon Ti. The generally low Ti_{apfu} among the isolated biotite inclusions is similar to that of the matrix biotite, although a direct chemical exchange with the outside environment is unlikely given the lack of effect on the Mg#.

Isolated inclusions as protolith mineralogy

Taking the isolated inclusion suite as a straightforward picture of the SVL gneiss' protolith mineralogy yields the picture of a granitoid containing quartz, exsolved K-feldspar and plagioclase, biotite, apatite, and minor Fe–Ti oxides and other phases. If occurrence rate in the zircons is indicative of modal mineralogy in the whole rock, then the protolith consisted of 25 % quartz and 15 % each of K-feldspar and oligoclase—a composition that is relatively poor in quartz and feldspar compared to most granitoids. Certain inclusion phases may be found in igneous zircon in much higher proportions than in the host rock (e.g., apatite; Rasmussen et al. 2011; Jennings et al. 2011) and may account for this low total quartz + feldspar. In addition, the late crystallization of zircon in most intermediate to felsic magmas should be expected to bias the zircon inclusion suite toward later-forming phases, as indeed demonstrated in natural samples by Darling et al. (2009) and Jennings et al. (2011). Instead of monzogranitic, the protolith may instead have been more granodioritic or dioritic in character.

The accessory mineralogy of the whole rock is only partially reflected in the zircon inclusion assemblage. Apatite, ilmenite, and titanite are abundant in the rock. The characteristic mantling of ilmenite by titanite (e.g., Fig. 2b, d) may suggest that titanite is a metamorphic phase formed through reaction of ilmenite with surrounding phases, although titanite is also a magmatic phase in many granitoids. While apatite is a minor inclusion phase, titanite was not observed in the inclusion assemblage. Ilmenite was observed in one zircon, but Fe–Ti oxides in other grains were more ambiguous in character.

Implications for zircon inclusion studies

The abundant mineral inclusions in zircon of the SVL orthogneiss include a secondary mineralizing assemblage similar to the main phases in the present rock (largely quartz, biotite, and albite) and a likely primary, igneous assemblage (most inclusions isolated from cracks). Mineral inclusions in zircon have usually been studied in the context of reconstructing P–T histories in metamorphic terranes (e.g., Liu and Liou 2011; Liu et al. 2001), but inclusion studies in detrital zircons may also provide important insights into sediment provenance, including some less accessible periods of Earth history. Inclusions in the 3.0–4.4 Ga Jack Hills zircons, for instance, are dominantly granitic (Bell et al. 2015b; Hopkins et al. 2008, 2010; Maas et al. 1992). Along with other geochemical characteristics, this has been interpreted as evidence for their origin in granitic rather than more mafic magmas (Hopkins et al. 2008, 2010; Maas et al. 1992), although Rasmussen et al. (2011) concluded that many of the inclusions were likely secondary, having precipitated from fluids that invaded the zircons along cracks, metamict regions, or unspecified "cryptic pathways." Resolution of this issue will be crucial to addressing the usefulness of Hadean mineral inclusions to understanding early Earth, including the investigation of rare carbonaceous inclusions which may shed light on the Hadean carbon cycle (Bell et al. 2015a).

This study of mineral inclusions in non-metamict zircons that have demonstrably undergone secondary mineralization since their formation can help to parse some of these potential obstacles to inclusion preservation. Cracks provide a clear path for fluid ingress into the zircons, and indeed the modal mineralogy of phases along cracks seems to be intermediate between that of the crack-isolated (likely primary) inclusions and the secondary assemblage seen filling cracks. Crack-intersecting feldspars include nearly pure albite, a relative lack of K-feldspar compared to the primary assemblage, and a complete lack of perthitic K-feldspar/plagioclase pairs, likely reflecting albitization. The moderate U contents are unlikely to have led to metamictization in most zircons over the gneiss's ca. 1 Ga history, and CL-dark regions often associated with radiation-damaged, high-U zircon are rare (see Table S1). For the most part, mineralogical and chemical differences in the isolated inclusion suite have little relationship with the pristinity of CL zoning or the U–Pb system, although 4 % (4 inclusions) of the isolated assemblage contains clearly metamorphic phases (chlorite, muscovite, epidote), three of the four residing in isotopically disturbed regions. Absent this isotopic evidence for volume alteration, there appears little role for fluid ingress apart from cracks. The majority of regions with disturbed zoning or U–Pb systems show little evidence for inclusion alteration, especially among plagioclase which appears to have mostly altered readily along cracks. Biotite chemistry

is an interesting case, in that like the other isolated inclusions the biotite is likely originally magmatic, although its low, matrix-like Ti_{apfu} is puzzling.

However, it appears clear that alteration of the majority of inclusions in these zircons was restricted to the regions immediately adjacent to cracks or to a few zircons with isotopic signs of alteration. Although disturbed CL zoning shows that some process has altered the host zircon in the regions surrounding these primary inclusions, this alteration did not appear to affect the chemistry or mineralogy of the inclusion itself. Further study may help to elucidate the nature of this alteration and to better predict modes of host zircon alteration that will or will not indicate a danger of inclusion alteration. A limitation of this study is the lack of preserved, unmetamorphosed SVL gneiss protolith, whose mineralogy and mineral chemistry could be compared to those of the isolated zircon inclusion assemblage.

The zircons in this study have preserved primary mineral inclusions even though later alteration of their host rock and mineralization of their cracks. It is likely that zircons in similar settings preserve their primary inclusion assemblages as well, in the absence of clear pathways for fluid ingress such as cracks or metamict regions. Further studies of inclusion-bearing zircon with varying degrees of radiation damage may be needed to determine the limits of this preservation potential and its applicability to important records such as the Jack Hills zircons. Future investigations of secondary mineralizing suites in zircon may also help to establish whether secondary assemblages are useful recorders of later host rock mineralogy or the composition of mineralizing fluids: The secondary assemblage in this study includes the majority phases in the present SVL gneiss but few of the accessories (apatite, titanite), which may not have been mobile.

Conclusions

Zircons in both the melanocratic majority and local leucosomes of a 1020 ± 13 Ma orthogneiss were investigated to assess the effect of later metamorphism and alteration on their mineral inclusion assemblages. The zircons are non-metamict and display characteristics consistent with an originally igneous nature, including igneous Th/U and Ti contents and originally magmatic (if in many cases later altered) CL zoning. The mineralogy and chemistry of the zircons' abundant mineral inclusions show no clear relationship with the unit (melanocratic, leucosome) from which the zircons were separated, nor with residence in magmatic or altered CL zoning in the host zircon. Inclusions intersecting cracks chemically and mineralogically resemble both the secondary mineralizing assemblage seen in void space along cracks in the zircons and also the main phases in the whole rock. Inclusions isolated from cracks preserve 4 % clearly metamorphic inclusions (mostly in isotopically disturbed regions), but elsewhere are characterized by phases consistent with igneous origins, including prominent K-feldspar/plagioclase pairs and feldspar and biotite compositions not seen in the secondary assemblage or the present whole rock, with the plagioclase compositions unlikely to have formed during Grenville metamorphism due to their relatively sodic nature compared to plagioclase in other (presumably less overprinted) regional gneisses (Bartholomew 1981). It appears that alteration of zircon mineral inclusions during amphibolite to lower granulite facies metamorphism (and a later greenschist facies overprint) in this orthogneiss occurred almost entirely along cracks, which served as pathways for fluid ingress. It is likely that other non-metamict zircons behave similarly, preserving primary igneous mineral inclusions during later metamorphism. Preservation of a secondary mineralizing assemblage, as in the likely greenschist facies phases filling cracks in these zircons, may also yield additional information in interpreting detrital or other zircons that have undergone metamorphic or metasomatic alteration.

Acknowledgments I thank Frank Kyte and Rosario Esposito for assistance with the EPMA analyses, Axel Schmitt and Rita Economos for assistance with the ion microprobe analyses, Julia and Martha Ann Bell for field assistance, and Matthew Wielicki for preparing the XRF analyses. Mark Harrison and Patrick Boehnke provided detailed and insightful comments on a first draft of this manuscript. Comments from the editor, Calvin Miller, and an anonymous reviewer greatly improved the manuscript. The ion microprobe facility at UCLA is partly supported by a grant from the Instrumentation and Facilities Program, Division of Earth Sciences, National Science Foundation. This research was supported by a Simons Collaboration on the Origins of Life Postdoctoral Fellowship (293529) to E.A.B.

Compliance with ethical standards

Conflict of interest The author declares that she has no conflict of interest.

References

Abbott SS, Harrison TM, Schmitt AK, Mojzsis SJ (2012) Ti–U–Th–Pb depth profiling of Hadean zircons: a search for evidence of ancient extraterrestrial impacts. Proc Natl Acad Sci 109:13486–13492

Bartholomew MJ (1981) Geology of the Roanoke and Stewartsville quadrangles, Virginia, vol 34. Commonwealth of Virginia, Dept. of Conservation and Economic Development, Division of Mineral Resources Publication, Richmond, VA, USA, p 23

Bartholomew MJ, Lewis SE (1984) Evolution of Grenville massifs in the Blue Ridge geologic province, southern and central Appalachians. In: Bartholomew MJ (ed) The Grenville event in the Appalachians and related topics, vol 194. Geological Society of America Special Paper, Boulder, CO, USA, pp 229–254

Bartholomew MJ, Gathright TM, Henika WS (1981) A tectonic model for the Blue Ridge in central Virginia. Am J Sci 281:1164–1183

Bell EA, Harrison TM, McCulloch MT, Young ED (2011) Early Archean crustal evolution of the Jack Hills Zircon source terrane

inferred from Lu–Hf, $^{207}Pb/^{206}Pb$, and $\delta^{18}O$ systematics of Jack Hills zircons. Geochim Cosmochim Acta 75:4816–4829

Bell EA, Boehnke P, Harrison TM, Mao WL (2015a) Potentially biogenic carbon preserved in a 4.1 billion year old zircon. Proc Natl Acad Sci 112:14518–14521

Bell EA, Boehnke P, Hopkins MD, Harrison TM (2015b) Distinguishing primary and secondary inclusion assemblages in Jack Hills zircons. Lithos 234:15–26

Boehnke P, Watson EB, Trail D, Harrison TM, Schmitt AK (2013) Zircon saturation re-revisited. Chem Geol 351:324–334

Cathelineau M (1986) The hydrothermal alkali metasomatism effects on granitic rocks: quartz dissolution and related subsolidus changes. J Petrol 67:945–965

Claiborne LL, Miller CF, Wooden JL (2010) Trace element composition of igneous zircon: a thermal and compositional record of the accumulation and evolution of a large silicic batholith, Spirit Mountain, Nevada. Contrib Mineral Petrol 160:511–531

Corfu F, Hanchar JM, Hoskin PWO, Kinny P (2003) Atlas of zircon textures. In: Hanchar JM, Hoskin PWO (eds) Zircons reviews in mineralogy and geochemistry, vol 53. Mineralogical Society of America, Washington, DC, USA, pp 469–500

Darling J, Storey C, Hawkesworth C (2009) Impact melt sheet zircons and their implications for the Hadean crust. Geology 37:927–930

Dobrzhinetskaya L, Wirth R, Green H (2014) Diamonds in Earth's oldest zircons from Jack Hills conglomerate, Australia, are contamination. Earth Planet Sci Lett 387:212–218

Engvik AK, Putnis A, Fitzgerald JD, Austrheim A (2008) Albitizatoin of granitic rocks: the mechanism of replacement of oligoclase by albite. Can Mineral 46:1401–1415

Fedo CM, Sircombe KN, Rainbird RH (2003) Detrital zircon analysis of the sedimentary record. In: Hanchar JM, Hoskin PWO (eds) Zircons reviews in mineralogy, vol 53. Mineralogical Society of America, Washington, DC, USA, pp 277–303

Fokin MA (2003) Space-time analysis of magmatism: the igneous record for an early Cryogenian plume track in central Appalachian orogen. M.S. Thesis, Virginia Polytechnic Institute and State University

Fu B, Page FZ, Cavosie AJ, Fournelle J, Kita NT, Lackey JS, Wilde SA, Valley JW (2008) Ti-in-zircon thermometry: applications and limitations. Contrib Mineral Petrol 156:197–215

Furcron AS (1969) Late Precambrian and early Paleozoic erosion-depositional sequences of northern and central Virginia: Georgia Geological Survey Bulletin 80, pp 57–88

Garver JI, Kamp PJJ (2002) Integration of zircon color and zircon fission-track zonation patterns in orogenic belts: application to the Southern Alps, New Zealand. Tectonophysics 349:203–219

Glover L III, Speer JA, Russell GS, Farrar SS (1982) Ages of regional metamorphism and ductile deformation in the central and southern Appalachians. Lithos 16:223–245

Harrison TM, Schmitt AK (2007) High sensitivity mapping of Ti distributions in Hadean zircons. Earth Planet Sci Lett 261:9–19

Harrison TM, Watson EB, Aikman AB (2007) Temperature spectra of zircon crystallization in plutonic rocks. Geology 35:635–638

Henika WS (2011) Geologic map of the Hardy quadrangle, Virginia. Virginia Division of Geology and Mineral Resources Open File Report 2011-3

Henry DJ, Guidotti CV (2002) Ti in biotite from metapelitic rocks: temperature effects, crystall-chemical controls and petrologic applications. Am Mineral 87:375–382

Henry DJ, Guidotti GV, Thomson JA (2005) The Ti-saturation surface for low-to-medium pressure metapelitic biotites: implications for geothermometry and Ti-substitution mechanisms. Am Mineral 90:316–328

Hopkins M, Harrison TM, Manning CE (2008) Low heat flow inferred from >4 Gyr zircons suggests Hadean plate boundary interactions. Nature 456:493–496

Hopkins M, Harrison TM, Manning CE (2010) Constraints on Hadean geodynamics from mineral inclusions in >4 Ga zircons. Earth Planet Sci Lett 298:367–376

Hoskin PWO, Schaltegger U (2003) The composition of zircon and igneous and metamorphic petrogenesis. In: Hanchar JM, Hoskin PWO (eds) Zircons Reviews in mineralogy and geochemistry, vol 53. Mineralogical Society of America, Washington, DC, USA, pp 27–62

Jennings ES, Marschall HR, Hawkesworth CJ, Storey CD (2011) Characterization of magma from inclusions in zircon: apatite and biotite work well, feldspar less so. Geology 39:863–866

Liu FL, Liou JG (2011) Zircon as the best mineral for P–T-time history of UHP metamorphism: a review on mineral inclusions and U–Pb SHRIMP ages of zircons from the Dabie–Sulu UHP rocks. J Asian Earth Sci 40:1–39

Liu J, Ye K, Maruyama S, Cong B, Fan H (2001) Mineral inclusions in zircon from gneisses in the ultrahigh-pressure zone of the Dabie mountains, China. J Geol 109:523–535

Maas R, Kinny PD, Williams IS, Froude DO, Compston W (1992) The Earth's oldest known crust: a geochronological and geochemical study of 3900–4200 Ma old detrital zircons from Mt. Narryer and Jack Hills, Western Australia. Geochim Cosmochim Acta 56:1281–1300

Menneken M, Nemchin AA, Geisler T, Pidgeon RT, Wilde SA (2007) Hadean diamonds in zircon from Jack Hills, Western Australia. Nature 448:917–920

Mojzsis SJ, Devaraju TC, Newton RC (2003) Ion microprobe U-Pb age determinations on zircon from the late Archean granulite facies transition zone of southern India. J Geol 111:407–425

Nemchin AA, Whitehouse MJ, Menneken M, Geisler T, Pidgeon RT, Wilde SA (2008) A light-carbon reservoir recorded in zircon-hosted diamond from the Jack Hills. Nature 454:92

Paces JB, Miller JD (1993) Precise U-Pb ages of Duluth complex and related mafic intrusions, northeastern Minnesota: geochronological insights to physical, petrogenetic, paleomagnetic, and tectonomagmatic processes associated with the 1.1 Ga midcontinent rift system. J Geophys Res Solid Earth 98:13997–14013

Plumper O, Putnis A (2009) The complex hydrothermal history of granitic rocks: multiple feldspar replacement reactions under subsolidus conditions. J Petrol 50:967–987

Rasmussen B, Fletcher IR, Muhling JR, Gregory CJ, Wilde SA (2011) Metamorphic replacement of mineral inclusions in detrital zircon from Jack Hills, Australia: implications for the Hadean Earth. Geology 39:1143–1146

Robinson MS (1976) Paleozoic metamorphism of the Piedmont-Blue Ridge boundary region in west-central Virginia: evidence from K–Ar dating. Geol Soc Am Abs Progr 8:257–258

Sinha AK (1976) Timing of metamorphic and igneous events in the central Piedmont and Blue Ridge. Geol Soc Am Abs Progr 8:267

Spear FS (1995) Metamorphic phase equilibria and pressure-temperature-time paths. Mineralogical Society of America, Washington, DC, USA

Trail D, Mojzsis SJ, Harrison TM, Schmitt AK, Watson EB, Young ED (2007) Constraints on Hadean zircon protoliths from oxygen isotopes, REEs and Ti-thermometry. Geochem Geophys Geosyst 8:Q06014

Watson EB, Harrison TM (2005) Zircon thermometer reveals minimum melting conditions on earliest Earth. Science 308:841–844

Wayne DM, Sinha AK (1988) Physical and chemical response of zircons to deformation. Contrib Mineral Petrol 88:109–121

Weber WJ, Ewing RC, Wang L-M (1993) The radiation-induced crystalline-to-amorphous transition in zircon. J Mater Res 9:688–698

Wiedenbeck M, Hanchar JM, Peck WH, Sylvester P, Valley J, Whitehouse M, Kronz A, Morishita Y, Nasdala L (2004) Further characterisation of the 91500 zircon crystal. Geostand Geoanal Res 28:9–39